Design on a highly birefringent and nonlinear photonic crystal fiber in the C waveband*

Li Duan-Ming(李端明)[a], Zhou Gui-Yao(周桂耀)[a)b)†], Xia Chang-Ming(夏长明)[a], Wang Chao(王 超)[b], and Yuan Jin-Hui(苑金辉)[a]

[a)] *Laboratory of Nanophotonic Functional Materials and Devices, South China Normal University, Guangzhou* 510006, *China*
[b)] *State Key Laboratory of Metastable Materials Science and Technology, Yanshan University, Qinhuangdao* 066004, *China*

(Received 19 May 2013; revised manuscript received 25 June 2013; published online 10 February 2014)

In this paper, a novel photonic crystal fiber (PCF) with high birefringence and nonlinearity is designed. The characteristics of birefringence, dispersion and nonlinearity are studied by using the full-vector finite element method (FVFEM). The numerical results show that the phase birefringence and nonlinear coefficient of PCF can be up to 4.51×10^{-3} and 32.8972 $W^{-1}\cdot km^{-1}$ at 1.55 μm, respectively. The proposed PCF could be found to have important applications in the polarization-dependent nonlinear optics such as the pulse compress and reshaping in the C waveband.

Keywords: high birefringence, nonlinear coefficient, zero dispersion wavelength, full-vector finite element method

PACS: 42.81.Gs, 42.65.–k, 42.81.–i **DOI:** 10.1088/1674-1056/23/4/044209

1. Introduction

Recently, photonic crystal fiber (PCF)[1–4] has become well known for its special optic properties, such as high birefringence,[5,6] high nonlinearity,[7,8] controllable dispersion,[9,10] etc. These characteristics make it appropriate for extensive use in optical fiber sensing, high power fiber laser, etc. Among these properties, high birefringence (HB) is required in fiber sensing to maintain the linear polarization by reducing polarization coupling. To reach a large difference in index, some HB PCFs have been reported by introducing an asymmetric structure, such as changing the air hole diameters along the two orthogonal directions,[11] introducing an asymmetric core,[12] and designing an elliptical-hole.[13] These HB PCFs have been reported to reach an order magnitude of 10^{-3} which is higher than the traditional HB fiber (10^{-4}).[14]

Highly nonlinear PCFs with zero dispersion wavelengths (ZDWs) have many important applications for supercontinuum (SC) sources,[15] all-optical signal process, and optical parametric amplifiers (OPA).[16] Because of these reasons, much work has concentrated on highly nonlinear PCFs, ZDW located around 1.55 μm. The theoretical design and simulation about this kind of PCF has been made by Ferrando *et al.*[17] Hansen *et al.*[18] first demonstrated this fiber with a 2.3-μm core (0.8-μm Ge-doped core inside), the nonlinear coefficient of 20 $W^{-1}\cdot km^{-1}$ and the birefringence order around 10^{-4}. Yamatmoto *et al.*[19] demonstrated a dispersion-flattened PCF (1.4 μm×1.1 μm Ge-doped elliptical core inside) with a modal birefringence of 1.3×10^{-3} and a nonlinear coefficient of 19 $W^{-1}\cdot km^{-1}$ at 1.55 μm. Compared with the Ge-doped optical fiber, the silica-core PCF with high birefringence and nonlinearity could be reached with a unique structure. Zhang[20] designed a PCF, which has a high nonlinearity of 105 $W^{-1}\cdot km^{-1}$ and confinement loss of lower than 10^{-2} dB/m in communication windows for generating broadband SC. Olyaee *et al.*[21] demonstrated a PCF, which has an effective mode area of 2.6 μm^2 and a confinement loss of 2.303×10^{-6} dB/km around 1.55 μm for an optical communication system. Zhang *et al.*[22] also reported on a PCF consisting of a central defect core and cladding with elliptical air holes, which has a low dispersion of ±2.5 $ps\cdot nm^{-1}\cdot km^{-1}$ in the wavelength range from 1.43 μm to 1.8 μm and a birefringence of 2.5×10^{-3} for four-wave mixing. In this paper, we present a new type of high birefringence and nonlinearity PCF with two ZDWs for the pulse compressing and reshaping in the C waveband.

2. Design of DC-PCF

The cross section of the proposed fiber is shown in Fig. 1. The whole fiber is based on pure silica and the cladding consists of a hexagon lattice with circular air-holes. The diameter of each small hole and each big hole are d and D, respectively. The pitch between the holes is denoted as Λ. To keep high birefringence, the sizes of some holes beside the core are different from the others', they form a "double crescent" style to increase the stress element of one direction beside the core. The "double crescent" part d/Λ has a most important role in determining the dispersion curve, which is assumed to shift the second ZDW's location and a larger air-filling fraction D/Λ is

*Project partly supported by the State Major Basic Research Development Program of China (Grant No. 2010CB327604) and the National Natural Science Foundation of China (Grant No. 61377100).

†Corresponding author. E-mail: zguiyao@163.com

© 2014 Chinese Physical Society and IOP Publishing Ltd

surrounded outside, which is used to confine the loss. Also the back-scattering of the simulation area boundaries is taken into account, an efficient full-vector FEM is applied to PCF and an anisotropic perfectly matched layer (PML) is employed. To ensure the higher accuracy, the curvilinear hybrid edge/nodal element is used to prevent the phony results.[20] Hence the PML's thickness owns five layers of gridding and the number of curvilinear hybrid edge/nodal elements for the PCF cross section is close to 5^7.

As seen in Fig. 1(b), the DC-PCF has an endless-single mode at 1.55 μm and the energy is completely confined in the core. Figures 1(c) and 1(d) show the polarized mode fields of HE_{11}^x and HE_{11}^y, respectively. Because of the weak confinement in the x-axis direction, the two polarized mode energies permeate to this side and the mode fields each present an ellipse shape.

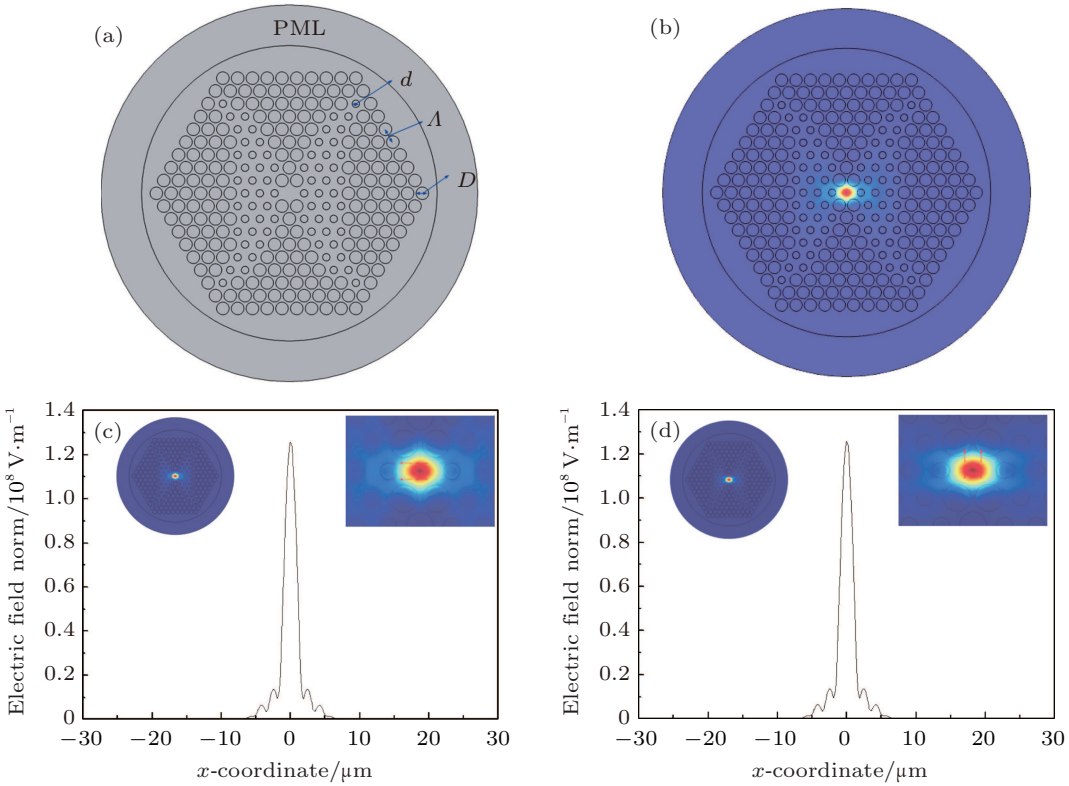


Fig. 1. (color online) (a) Cross section of the "double crescent" photonic crystal fiber, (b) fundamental mode field at 1.55 μm, (c) and (d) polarized mode fields of (c) HE_{11}^x and (d) HE_{11}^y, respectively.

3. Simulation results and discussion

As mentioned above, modal birefringence (B) property as a function of wavelength is investigated. The value of B is obtained according to the following formula

$$B = \frac{|\beta_x - \beta_y|}{k} = \left|\mathrm{Re}\left(n_{\mathrm{eff}}^x(\lambda)\right) - \mathrm{Re}\left(n_{\mathrm{eff}}^y(\lambda)\right)\right|. \quad (1)$$

Here, $n_{\mathrm{eff}x}$ and $n_{\mathrm{eff}y}$ are the effective refractive indices of the orthogonal polarization fundamental modes. The cruces of variables for Λ are shown in Fig. 2(a), where the d/Λ and D/Λ are fixed at 0.5Λ and 0.85Λ, respectively. The birefringence increases with the wavelength increasing and gradually increases to the maximum, then decreases. The maximum birefringence wavelength has a red shift with the increasing of Λ. This is due to the fact that a larger Λ means a larger core and cladding which could have more powerful constraints on a long wavelength. As seen in Fig. 2(b), to investigate the birefringence variation along the HE_{11}^x direction, we fix d/Λ at 0.5 and change D/Λ from 0.8 to 0.9 in steps of 0.05 with $\Lambda = 1.71$ μm. The maximum birefringence wavelength has a blue shift with the increasing of D/Λ. From Fig. 2, when $\Lambda = 1.71$ μm, $d/\Lambda = 0.5$, and $D/\Lambda = 0.85$, the DC-PCF reaches a birefringence of 4.51×10^{-3} at 1.55 μm in the C waveband which is higher than that reported in Refs. [11] and [23].

Due to the fact that the chromatic dispersion is associated with the PCF information carrying capacity and the generation of SC, it is necessary to investigate the dispersion of the DC-PCF. The chromatic dispersion is defined as

$$D(\lambda) = D_{\mathrm{w}}(\lambda) + D_{\mathrm{m}}(\lambda) = -\frac{\lambda}{c}\frac{\partial^2 n_{\mathrm{m}}}{\partial \lambda^2} - \frac{\lambda}{c}\frac{\partial^2 |R_{\mathrm{e}}(n_{\mathrm{eff}})|}{\partial \lambda^2}, \quad (2)$$

where $\mathrm{Re}(n_{\mathrm{eff}})$ is the real part of n_{eff}, n_{m} is based on λ in the dispersive medium and calculated by Sell Meier' s formula, c is the velocity of light in the vacuum, $D_{\mathrm{m}}(\lambda)$ is the material dispersion, and $D_{\mathrm{w}}(\lambda)$ is the waveguide dispersion.

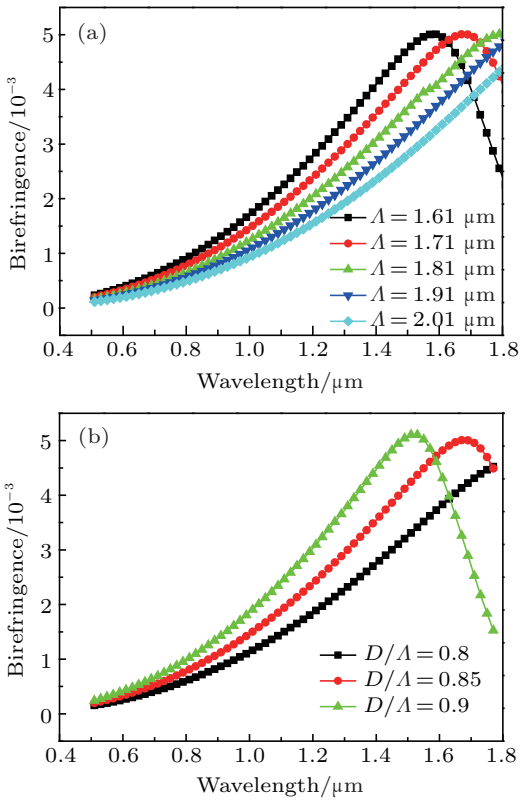


Fig. 2. (color online) (a) Variation effect of Λ on the birefringence by fixing the d/Λ and D/Λ values at 0.5 and 0.85, respectively. (b) Variation effect of D/Λ on the birefringence by fixing the d/Λ and Λ values at 0.5 and 1.71 μm, respectively.

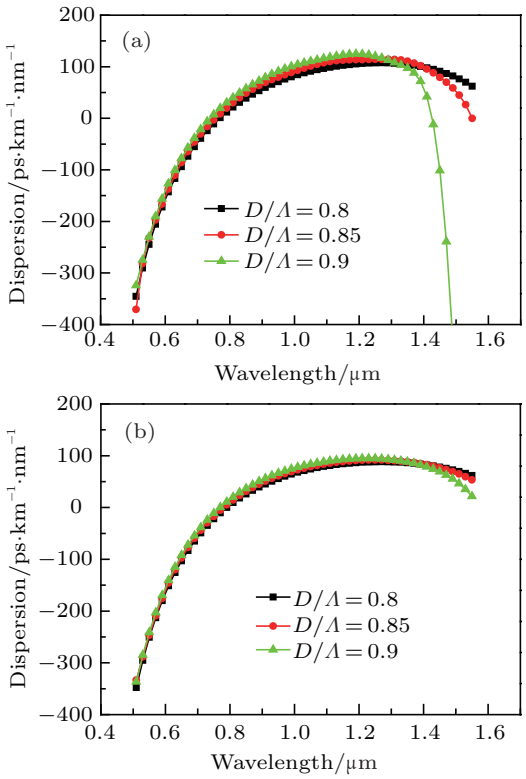


Fig. 3. (color online) Variation effects of D/Λ on the PCF chromatic dispersion along (a) HE_{11}^{x} and (b) HE_{11}^{y} by fixing $\Lambda = 1.71$ μm, $d/\Lambda = 0.5$.

The wavelength-dependent properties of chromatic dispersion $D(\lambda)$ are represented in Figs. 3 and 4, while the silica index is assumed to be 1.45. In Fig. 3, the curves show the chromatic dispersions by fixing $\Lambda = 1.71$ μm, $d/\Lambda = 0.5$, and they are calculated at different values of D/Λ. There are two ZDWs in the visible wavelength band and the near infrared band, respectively. The first ZDW is located in the working wave band of the Ti:sapphire oscillator (700 nm–980 nm) which could contribute to the Ti:sapphire femtosecond laser frequency conversion and it shifts toward the short wave with D/Λ changing from 0.8 to 0.9 in the steps of 0.05.

As shown in Fig. 4, there is a clear trend in the near infrared band, showing that the second ZDW moves to the long wavelength by increasing the d/Λ. The difference between the dispersion curves at the long wavelengths also becomes clearer at the various values of d/Λ. When $d/\Lambda = 0.5$, $D/\Lambda = 0.85$, and $\Lambda = 1.71$ μm, the short wave ZDW is around 760 nm and the near infrared ZDW is at 1.55 μm.

The influence of Λ on chromatic dispersion is also considered as shown in Fig. 5. A significant difference between HE_{11}^{x} and HE_{11}^{y} appears in the long wave band. This is because the low air-filling fraction at the x axis surrounds the core and the wavelength approaches the value of Λ, which leads to a weak confinement on the energy. The second ZDW wavelength has a red shift with the increasing of Λ.

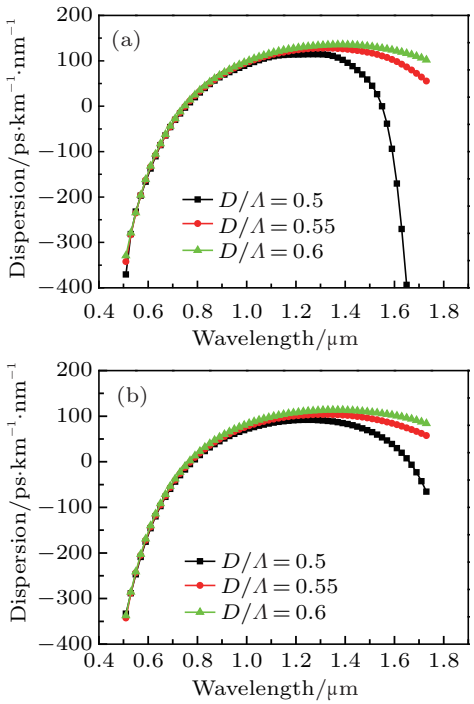


Fig. 4. (color online) Variation effects of d/Λ on the PCF chromatic dispersion along (a) HE_{11}^{x} and (b) HE_{11}^{y} by fixing $\Lambda = 1.71$ μm, $D/\Lambda = 0.85$.

In Fig. 6, the chromatic dispersion and the nonlinear coefficient are considered each as a function of wavelength, by fixing $D/\Lambda = 0.85$, $d/\Lambda = 0.5$, and $\Lambda = 1.71$ μm. The non-

linear coefficient could be defined as

$$\gamma(\lambda) = \frac{2\pi n_2}{\lambda A_{\text{eff}}}. \tag{3}$$

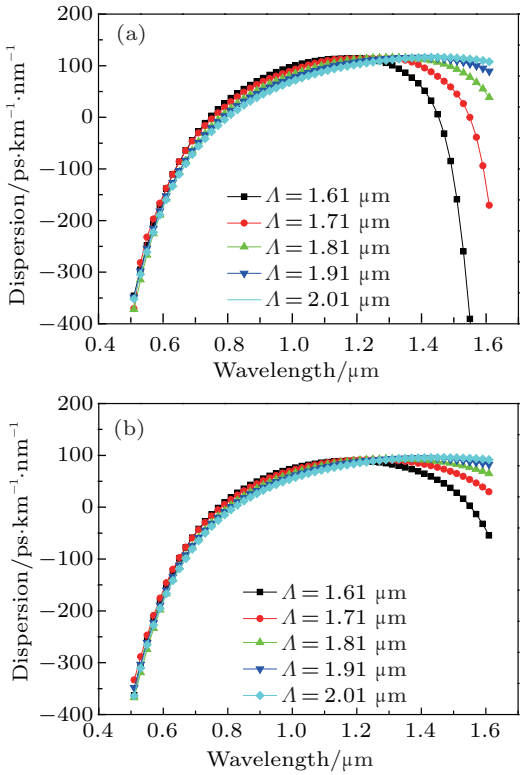


Fig. 5. (color online) Variation effects of Λ on the PCF chromatic dispersion along (a) HE_{11}^{x} and (b) HE_{11}^{y} by fixing $D/\Lambda = 0.85$, $d/\Lambda = 0.5$.

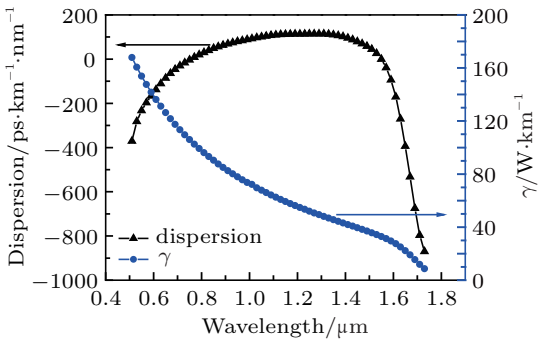


Fig. 6. (color online) Chromatic dispersion and the nonlinear coefficient each as a function of the wavelength for the DC-PCF with $D/\Lambda = 0.85$, $d/\Lambda = 0.5$, and $\Lambda = 1.71$ μm.

Here, the nonlinear refractivity n_2 of the pure silica material is 3.2×10^{-20} m^2·W^{-1},[24] and A_{eff} is the effective mode area. It could be seen that the nonlinear coefficient decreases with the increasing of wavelength, which is because of the powerless constraints on the long wavelength, thereby leading to a larger mode area. In Eq. (3), we can find that the larger mode area means a lesser nonlinear coefficient. As shown in Fig. 6, the nonlinear coefficient reaches 32.8972 W^{-1}·km^{-1} at 1.55 μm and the ZDW is also around here. The higher nonlinear coefficient and the particular ZDW have important applications in SC generation and telecommunication.

4. Conclusions

Based on the full-vector finite element method with an anisotropic perfect match layer, we design a DC-PCF which has a birefringence of 4.51×10^{-3} and a nonlinear coefficient of 32.8972 W^{-1}·km^{-1} at a zero dispersion wavelength of 1.55 μm. The proposed PCF offers a higher birefringence which is one order of magnitude higher than traditional fibers and increases the quality of the polarization with a higher nonlinear coefficient. These are conducible to optical fiber in pulse compressing and reshaping in the C waveband, soliton communication, and frequency transformation. The two ZDWs which are located in the working band of the Ti:sapphire oscillator (700 nm–980 nm) and communication band (C waveband), can be used for conversing the Ti:sapphire femtosecond laser frequency and broadening the SC spectrum.

References

[1] Knight J C, Birks T A, Russell P S J and Atkin D M 1996 *Opt. Lett.* **21** 1547
[2] Saitoh K, Koshiba M, Hasegawa T and Sasaoka E 2003 *Opt. Express* **11** 843
[3] Xiao L M, Birks T A and Loh W H 2011 *Opt. Lett.* **36** 4662
[4] Knight J C 2003 *Nature* **424** 847
[5] Ortigosa-Blanch A, Knight J C, Wadsworth W J, Arriaga J, Mangan B J, Birks T A and Rueesll P S J 2000 *Opt. Lett.* **25** 1325
[6] Ju J, Jin W and Demokan M S 2003 *IEEE Photon. Technol. Lett.* **15** 1375
[7] Tatsuya K, Yoshinori N, Kazuya A, Taito K, Shubi F K, Abdur Razzak S M, Begum F, Shinya N and Hiroki H 2010 *Opt. Rev.* **17** 61
[8] Finazzi V, Monro T M and Richardson D J 2003 *J. Opt. Soc. Am. B* **20** 1427
[9] Saitoh K, Florous N and Koshiba M 2005 *Opt. Express* **13** 8365
[10] Zografopoulos D C, Vázquez C, Kriezis E E and Yioultsis T V 2011 *Opt. Express* **19** 21680
[11] Xu Q, Miao R C and Zhang Y N 2013 *Optik* **124** 2269
[12] Xia C M, Zhou G Y, Han Y and Hou L T 2011 *Chin. Opt. Lett.* **9** 100609
[13] Tamura K, Ippen E P, Haus H A and Nelson L E 1993 *Opt. Lett.* **18** 1080
[14] Noda J, Okamoto K and Sasaki Y 1986 *J. Lightwave Technol.* **4** 1071
[15] Saitoh K and Koshiba M 2004 *Opt. Express* **12** 2027
[16] Poli F, Adami F, Foroni M, Rosa L, Cucinotta A and Selleri S 2005 *Appl. Phys. B* **81** 251
[17] Ferrando A, Silvestre E, Andres P, Miret J and Andres M 2001 *Opt. Express* **9** 687
[18] Hansen K P, Jensen J R, Jacobsen C, Simonsen H R, Jes Broeng, Skovgaard P M W and Petersson A 2002 *OFC*, Post Deadline FA9-1
[19] Yamamoto T, Kubota H, Kawanishi S, Tanaka M and Yamaguchi S 2003 *Opt. Express* **11** 1537
[20] Zhang Y N 2011 *Appl. Opt.* **50** E125
[21] Olyaee S, Taghipour F and Izadpanah M 2011 *Front. Optoelectron. China* **4** 420
[22] Zhang Y N, Ren L Y, Gong Y K, Li X H, Wang L R and Sun C D 2010 *Appl. Opt.* **49** 3208
[23] Kakarantzas G, Ortigosa-Blanch A, Birks T A, Rusell P S J, Farr L, Couny F and Managan B J 2003 *Opt. Lett.* **28** 158
[24] Xia C M, Zhou G Y, Han Y, Liu Z L and Hou L T 2011 *Acta Phys. Sin.* **60** 094213 (in Chinese)